Original Research Article

Photocatalytic Decomposition of Methylene Blue over Nanosized Ca^{2+} Doped $LaMnO_3$ under Visible Light Irradiation

ABSTRACT:

The Photocatalytic performance of the Calcium doped lanthanum manganite nanocomposite for photodegradation of Methylene Blue(MB) dye as an Organic water pollutant,was evaluated over visible light irradiation, at a pH of 4, at constant dose for several hours. The result showed $La_{0.75}Ca_{0.25}MnO_3$ having Perovskite structure shows high degree of catalytic efficiency of 69% within 100 min illumination time, for the removal of Methylene Blue organic dye from its aqueous solution. The sample powder(LCMO) was prepared through sol-gel technique and was characterized by X-ray diffraction (XRD), Fourier transform infrared spectroscopy (FTIR), Inductively coupled plasma- atomic emission spectroscopy (ICP-AES), Scanning electron microscopy (SEM), Energy dispersive X-ray spectroscopy (EDX) and UV-Vis spectroscopy (UV-Vis). The XRD data revealed the formation of single phase crystallinity.SEM images shows that the micro sized $La_{0.75}Ca_{0.25}MnO_3$ powder has nanocrystalline structure with average diameter of 1-3 µm. The ICP-AES data confirmed formation of required stoichiometric $La_{1-x}Ca_xMnO_3$ Oxide. The rates of photodegradation linearly increase as a function of time of irradiation, which was confirmed from study of the optical properties of the resulting aqueous solutions. These findings shows convincingly that $La_{0.75}Ca_{0.25}MnO_3$ photocatalyst possess great promise for visible light driven photodegadation of Methylene Blue dye.

Keywords: Perovskite, Sol-Gel technique, Photocatalyst, Methylene Blue.

1. INTRODUCTION

The wastewater discharges of industries cause serious environmental problems. Organic dyes in wastewater are the effective environmental pollutants whose removal causes a challenging issue. Intensive studies have been made on the Photocatalytic degradation of such dyes on the surface of metal oxides and it has been found that semiconductor mediated heterogeneous photocatalysis is a promising technology to degrade a wide range of organic pollutants.[1–8] . Metal oxides such as TiO_2 can be used only in UV lights (<387nm) because of a large band gap of 3.2eV. Thus there is an urgent need for efficient semiconductor catalytic systems with a narrower band gap, which are effective under visible light irradiation or ambient conditions, for harvesting the sunlight.[9-10]. As reported [11,12], TiO_2 showed improved photocatalytic behaviour in the visible light by number of methods like metal or non-metal ion doping and composite semiconductor formation etc.

Oxides with Perovskite structures having general formula of ABO_3 (A is cations of large size, such as La, Ca, Ba, Sr, Pb, Nd, Pr,… ions; B is smaller cations such as Mn, Co, Cr, Fe,…ions), have been extensively studied as catalysts for number of processes in the visible region [13], because of their high thermal stability, low cost, and having a facile synthetic pathways. Perovskites are suitable catalysts for degradation of pollutants because of non-toxicity, ease of use, and high resistance against water, organic, acidic, and alkaline solvents. La-based Perovskies (e.g. $LaCoO_3$, $LaMnO_3$, and $LaFeO_3$) have been proved as safe and greener catalyst for the degradation of aqueous solution of methyl orange under various conditions [14-15], because their catalytic properties can be properly tuned by

substituting A-site atoms with other kinds of cations such as Sr, Ce, Ba, and Eu having environmental applications [16-17]. Manganites by nature are semiconductors and their photocatalytic behaviour is attributed to having an empty Conduction Band (CB) and a full Valence Band (VB) in their electronic structure [18,19]. According to Sun et al [20], the physical and chemical activity of these materials are caused by two fundamental factors: (1) A unit cell with a corner-shared BO_6 octahedron network that can promote electron hopping. Because of its high reducibility, ABO_3 molecule is a great catalyst for pollutant degradation. (2) The A-site atom of ABO_3 contribute to the stabilisation of multiple valence states of B site cations. This makes the electrons in ABO_3 oxides more active, allowing them to be quickly activated by an external cause such as light irradiation.

In this study, rate of the degradation of a model of organic pollutant, Methylene Blue (MB), was investigated over $La_{0.7}Ca_{0.3}MnO_3$ nano-perovskite under visible light irradiation. The A-site doping with calcium is supposed to decrease the band gap energy thereby causing changes in electrical and photocatalytic properties. In hope of keeping up with further development of the lanthanum manganite adsorptive characteristics and for getting the oxides in a cost effective way as the calcium reagent is less expensive than lanthanum reagent, the present study is carried out. The inclusion of a divalent soluble component into La destinations enormously changes the electronic and adsorptive characteristics of the parent compound by making openings in the singlet Mn state by changing some Mn^{+3} particles to Mn^{+4} [21].

2. METHODOLOGY:

$La_{0.75}Ca_{0.25}MnO_3$ (LCMO) was synthesized via autocombustion method by mixing Sigma Aldrich-USA, AR grade $La(NO_3)_3.6H_2O$, $Ca(NO_3)_2.4H_2O$ and $Mn(NO_3)_2.4H_2O$ as the raw chemicals in 0.75:0.25:1.0 molar ratio. Citric acid was added as 100% of total amount of the chemicals mixture solution for auto combustion followed by addition of 5ml of ethylene glycol as surfactant. The prepared mixture with p^H of 8, was stirred vigorously for next 30-45 min to get dark-brown gel. The viscous liquid so obtained was dried at 120^oC over night. The final powder was calcined at 800^oC for 6 hours in the Muffle furnace (Model No: AI-106).

X-ray diffraction (XRD), inductively coupled plasma-atomic emission spectroscopy (ICP-AES), field emission scanning electron microscopy (FESEM), Fourier transform infrared spectroscopy (FTIR), and UV-VIS absorption spectroscopy were used to investigate the structural, spectroscopic, and optical properties of the resulting powders..

The visible light induced photodegradation of aqueous Methylene Blue(MB) solution(5 ppm and pH = 4) by using Calcium doped Lanthanum manganite as photocatalyst(0.07g l^{-1}),was carried out at room temperature under magnetic stirring and irradiation of one 100 W fluorescent lamps as a visible-light source, 10cm above the surface of MB solution. The mixture of photocatalyst in water was ultrasonicated for 15 min. Since the highest efficiency in the photocatalytic activity has been reported in low pH[23,24], MB solution was added carefully with stirring during the photocatalysis process at constant pH= 3.5, The reaction mixture was allowed to be magnetically stirred in dark for 30 minutes to attain adsorption-desorption equilibrium of MB on the surface of catalyst. In appropriate intervals, 5 mL of suspensions was collected and centrifuged. The MB concentration was determined by using the UV–VIS spectrophotometer for both the samples in the dark and after light irradiation. The proportionate decrease in concentration of MB in the solution was used to investigate the activity of the LCMO particles.

3. RESULTS AND DISCUSSION:

3.1. TG-DTA Analysis

Thermogravimetric studies of the prepared sample at the heating rates of 5^0C/min from 30^0C to 1000^0C, was carried out using Schimadzu DTG 50 thermal analyser. The weight loss curve shows several steps of decomposition.The primary weight loss found between 57^0C to 150^0C is associated with loss of water.(Fig-1).

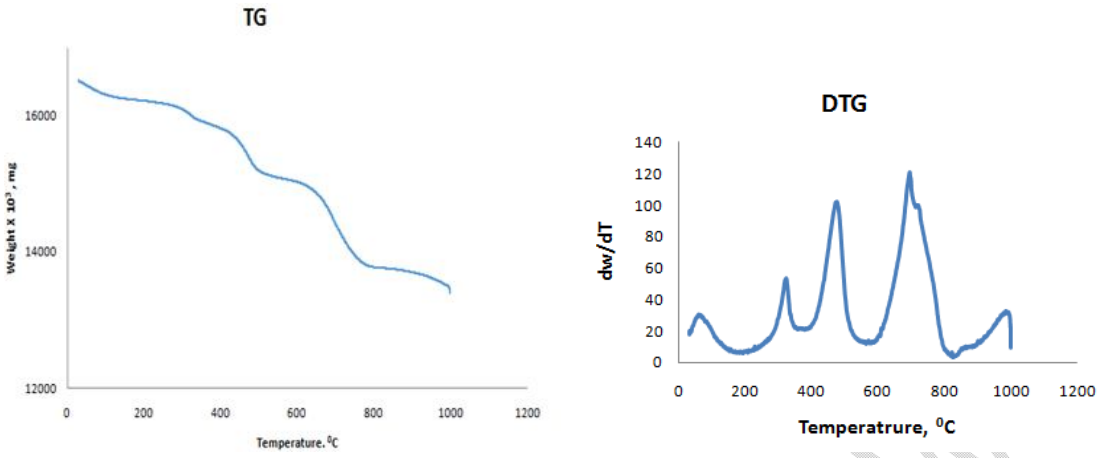

(Fig-1: TG and DTG curves of LCMO nano-perovskite)

A minor disintegration observed between 250^{0}C to 380^{0}Cwhich might occur due to breaking of polymeric chain. The second step weight loss between 400^{0}C to 570^{0}C is due to decomposition of nitrates and citrates and implies initial formation of LCMO nano perovskite. The final stage of mass degradation took place between 600^{0}C to 800^{0}C which is due to formation of phase pure or crystalline LCMO nano-perovskite. Above 800^0 there is a very weak mass degradation which shows completion of perovskite oxide phase formation.The prefixing of calcinations temperature was estimated from results of TGA analysis.

3.2. XRD Analysis:

Powder XRD (Fig-2) of the prepared $La_{0.75}Ca_{0.25}MnO_3$ (LCMO) sample was carried out by X-ray diffractometer (PAN Analytical Empyrean Series 2) with Cu Kα (λ = 0.15406nm) radiation in the 2θ range of 10^0 to 90^0 [Table-1], under current of 30mA and 40Kv.The synthesized sample has single-phase perovskite structure. The characteristic peak was obtained at 2θ value of 32.65^0. The data was analysed with the use of a commercial X-pert package and the FULLPROF programme. The X-pert high score PDF (code: 01-075-0440) matches the diffraction peaks, confirming the creation of a cubic LaMnO3 perovskite phase.

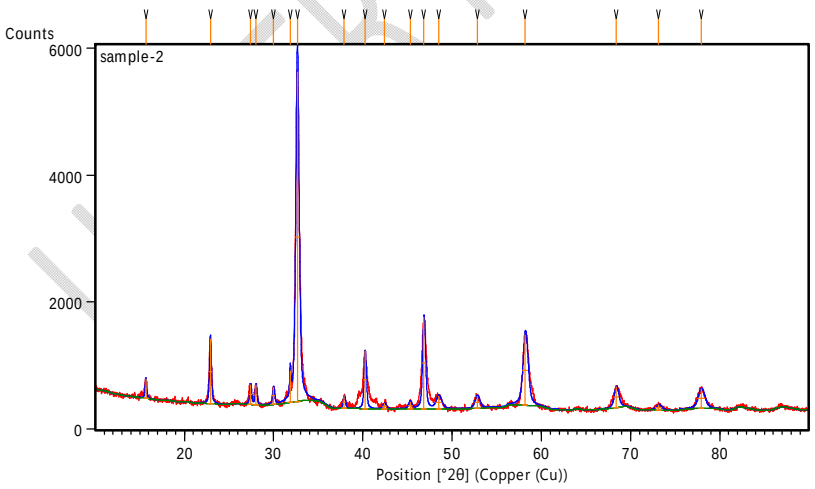

(Fig-2:XRD Pattern of the LCMO nano-perovskite sample)

The figure shows that the calcium doped sample gives broadened peaks which represent the smaller size of crystals in the compositions. The broadening of peak is because of finite size of the crystals.

Table-1: X- Ray Crystallographic data of $La_{0.75}Ca_{0.25}MnO_3$ nano-perovskite sample)

Pos. [°2θ]	d-spacing [Å]	Rel. Int. [%]
22.9058	3.88259	19.51
32.6502	2.74270	100.00
40.2325	2.24158	17.55
46.8260	1.94017	27.76
58.1931	1.58537	21.38

3.3. SEM Analysis:

Morphological studies of the prepared sample was carried out in HITACHI S-3400N scanning electron microscope. The SEM images [Fig. 3] demonstrate that the surface of the synthesised perovskite is porous, crooked, and rough with many cavities. The particle size and shapes vary as well. The excellent adsorptive properties are explained by this.

3.4. EDAX Analysis:

The surface atoms of the prepared LCMO sample were investigated quantitatively as part of the Energy Dispersive Analysis X-ray (EDAX) study [Fig-4]. The existence of La, Ca, Mn, and O atoms is what causes the corresponding peaks in the spectrum. The absence of additional impurity peaks demonstrates the natural purity of the synthesised sample. Likewise, the Atomic weight ratio of (La+Ca):Mn = 1.07, indicates the expected nature of stoichiometry of the prepared sample. [Table-2]

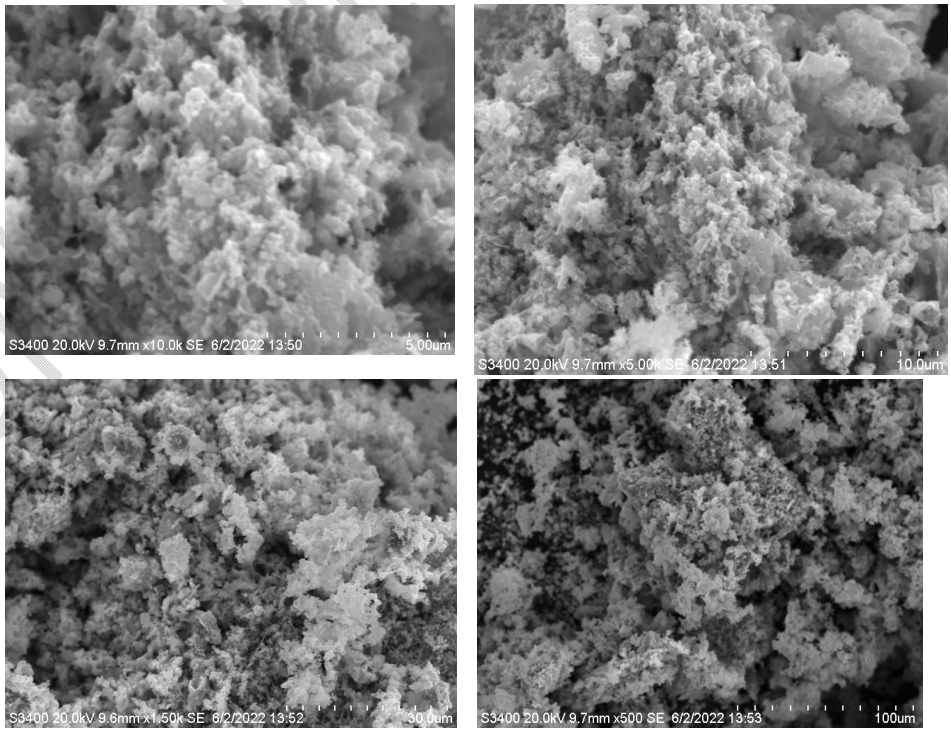

(Fig-3: SEM images of synthesized LCMO nano-perovskite)

[Table-2: EDAX elemental composition of synthesized LCMO sample]

Elements	Weight %	Atomic %
O K	13.73	52.57
Ca K	11.08	4.56
Mn K	23.77	22.85
La L	51.42	20.02
Total	100	100

.

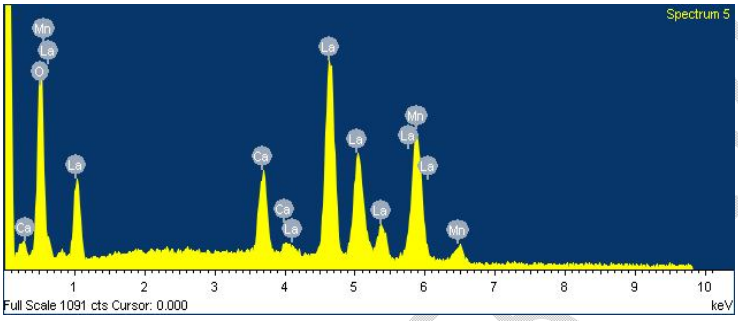

(Fig-4: EDAX Patterns of synthesized $La_{0.75}Ca_{0.25}MnO_3$ nano-perovskite)

3.5. FT-IR Analysis:

The FT-IR spectra of LCMO perovskite [Fig-5] was analysed by using PERKIN ELMER UATR 2, FT-IR spectrophotometer. The spectra shows peaks at 492.94 cm^{-1}, 586.40 cm^{-1}, 880.59 cm^{-1}, 1060.90 cm^{-1}, 1160.37 cm^{-1},3609.33 cm^{-1} etc. The main absorption band around 492.94 cm^{-1}, due to the bending mode of Mn-O-Mn bond. The absorption band at 586.40 cm^{-1} arises from the stretching mode of Mn-O-Mn bond which involves motion of a change in Mn-O-Mn bond length. Thus presence of both the peaks shows the strong metal-oxygen bond present in the sample. These two bands are related to the environment surrounding the MnO_6 octahedron in the ABO_3 perovskite and confirms the formation of perovskite structure, which is in agreement with the XRD results. The peak at 880.59 cm^{-1} is due to presence of atmospheric CO_2 whereas peaks at 1033.42 cm^{-1} and 1060.90 cm^{-1} are due to presence of little carbonates in the sample. Besides, the peak of 1427.6 cm^{-1} is related to the asymmetric elongation of O-C-O vibration. The absorption peak at 3609.33 cm^{-1} is due to -OH stretching of water particles absorbed or presence of unreacted $La(OH)_2$in the sample.

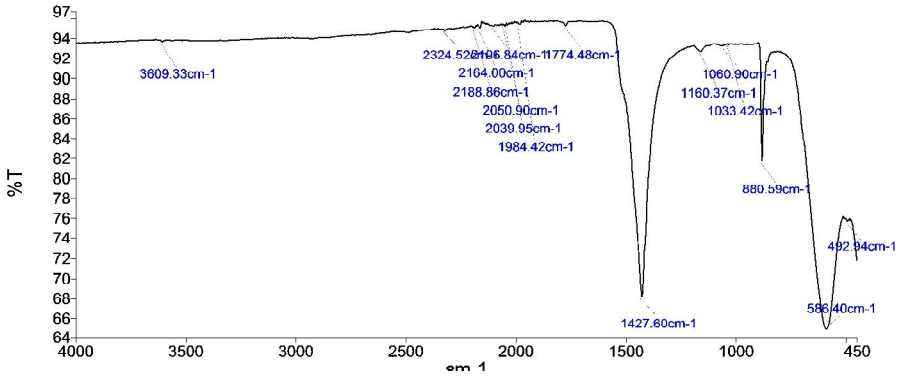

(Fig-5: FT-IR analysis of $La_{0.75}Ca_{0.25}MnO_3$ nano-perovskite)

3.6. ICP-AES Analysis:

The stichiometric proportions of the metal elements in the prepared sample was estimated by ICP-AES (THERMO iCAP 7000 series) analysis.The result concluded that the composition is close nearer to stoichiometry of the normal composition $La_{0.7}Ca_{0.3}MnO_3$ and it is named as $La_{0.74}Ca_{0.28}MnO_3$.

3.7. Optical properties:

Due to the optical response of the material, two conspicuous peaks (Fig-6) are visible. The first peak is found at approximately 235 nm (5.2 eV), and a high absorbance value is observed at approximately 325-380 nm (3.8-3.3 eV).The LCMO nanoparticles' band gap energy was calculated from the UV-VIS spectra using Tauc's plot of $(h\nu\alpha)^2$ vs $(h\nu)$.The linear portion of the curve is extrapolated to the energy axis using the following equation [21]:

$(\alpha h\nu)^2 = A(h\nu - E_g)$,

where α is the absorption coefficient, E_g the band gap energy, hν the photon energy and A the constant dependant on the effective masses of the electron, hole, and the material refractive index. The Tauc's plot of the sample is shown in Figure-7. The estimated optical band gap of $La_{0.74}Ca_{0.28}MnO_3$ nanowires is about 2.13 eV. Based on the band gap energy measurements, the synthesised samples are determined to be good candidates for employment as a photocatalyst [22].

The efficiency of degradation of MB is estimated as follows [25]:

$D\ \% = (A^0 - A) / A^0 \times 100$ (1)

Where A_0 and A represent the initial MB solution absorbance and absorbance at time t.

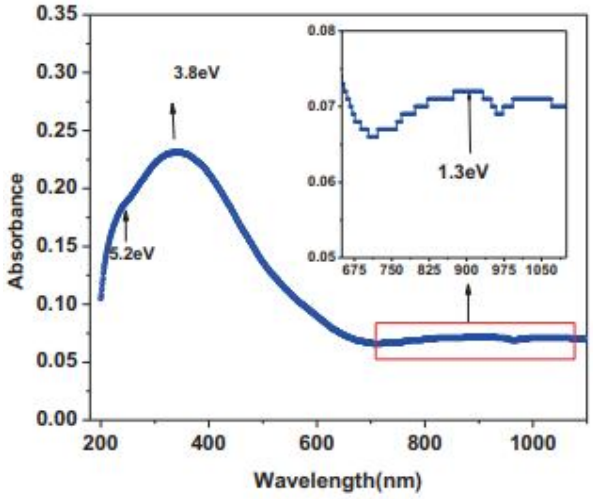

(Fig-6: UV-VIS spectrum of $La_{0.75}Ca_{0.25}MnO_3$ nano-perovskite)

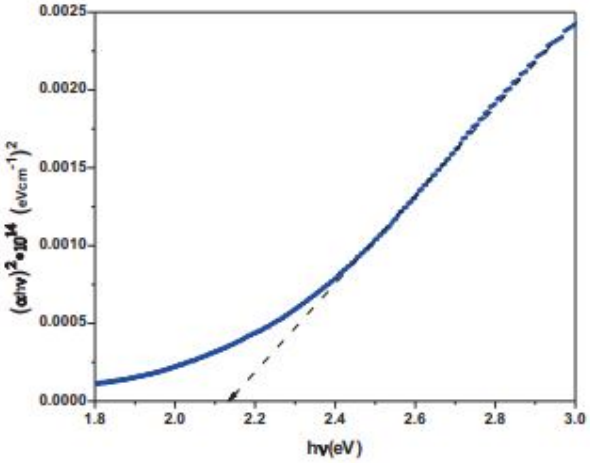

(Fig-7: Tauc's plot of the $La_{0.75}Ca_{0.25}MnO_3$ nano-perovskite)

Table-3: Percentage of Degradation of MB (Visible light and Dark)

TIME, min	% DEGRADATION	
	Visible Light	Dark
0	52.07	0.02
20	59.07	0.5
40	60.70	1.05
60	63.61	2.0
80	66.01	5.5
100	68.52	6.2

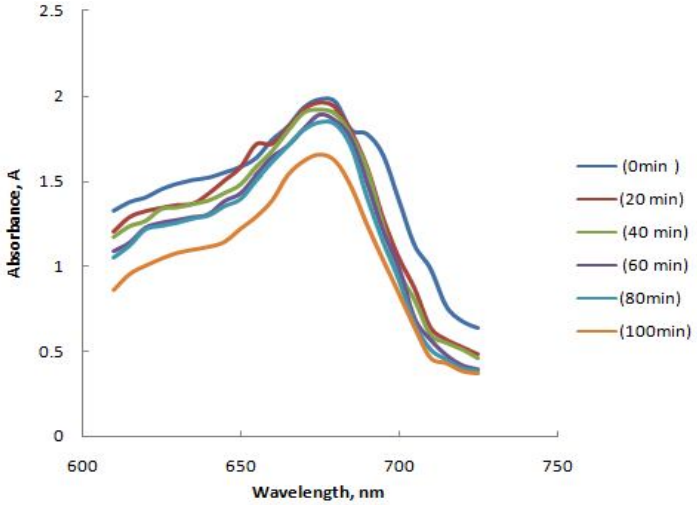

(Fig.8. UV-VIS absorption spectrum of MB at different time intervals in presence of LCMO)

The absorbance of MB solution decreases with increasing time of exposure to the light indicating the deceasing concentration and hence increase in degradation (Fig-8). The percentage of degradation increases with illumination time up to 100 minutes for all the samples(Fig-9) and a comparative study in dark is presented in Table-3. A shorter time interval is chosen in order to optimize the rate of degradation within a short period of time.

3.8. **Kinetics of photodegradation:**

Because chemical substitution influences two crucial photocatalytic activations parameters, namely the enhancement of the hole-doping level and the lowering of E_g , it is important to note that the kinetics of photodegradation follows the Langmuir-Hinshelwood equation [26]

$r = - (dC/dt) = k_{app}\, t$ (2)

where 'r' is the rate of degradation,'k_{app}' is the rate constant of reaction, and 'C' is the concentration of the reactant at time 't'.

Integration of this equation (with the restriction $C = C^0$ at $t = 0$ with C^0 being the initial concentration in the bulk solution in dark adsorption) will lead to equation (3):

$- \text{Ln} (C^t/C^0) = k_{app}\, t$ (3)

where C^0 is the primary concentration of MB, C^t is the concentration of Methylene Blue at the reaction time t

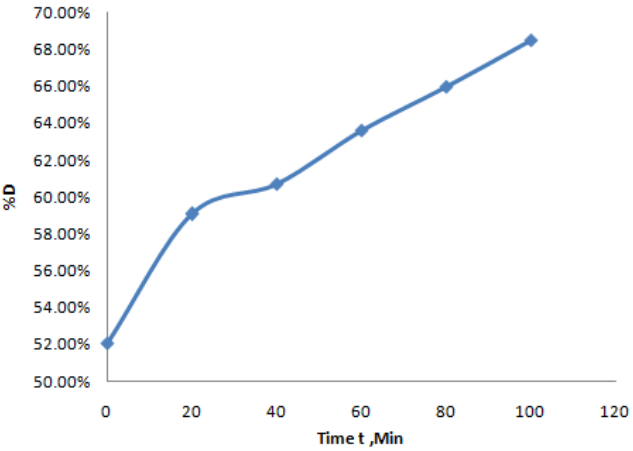

(Fig.9: % Degradation of Methylene Blue using $La_{0.75}Ca_{0.25}MnO_3$ under visible light irradiation)

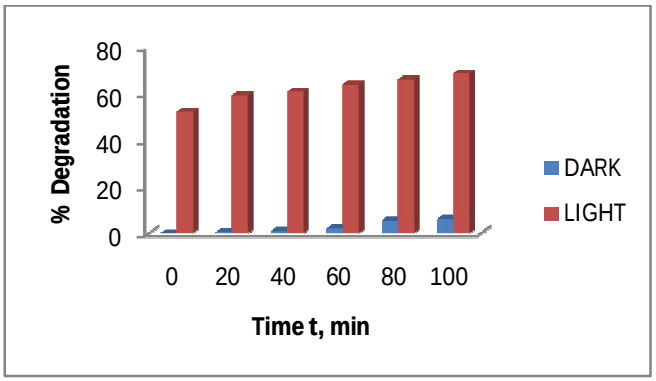

(Fig. 10. Degradation profile of MB in presence of $La_{0.75}Ca_{0.25}MnO_3$ under dark and visible light irradiation)

Since the concentration of MB solution is directly proportional to the absorbance, the pseudo first order rate constant , k_{app} is estimated from the slope of the liner plot(Fig-11), which was found to be 1.582 $x10^{-3}$ min^{-1} using $La_{0.7}Ca_{0.3}MnO_3$ perovskite as photocatalyst.

By substituting La^{3+} with a divalent Ca^{2+}cation, Mn^{4+} ions can be introduced [27].Thus $La_{1-x}Ca_xMnO_3$ compounds belongs to the category of hole-doped manganite perovskites. Since the mother sample ($LaMnO_3$) is Mn^{3+} rich, $La_{1-x}Ca_xMnO_3$ ($La^{3+}{}_{1-x}Ca^{2+}{}_x$ $Mn^{3+}{}_{1-x}Mn^{4+}{}_x$ O_3) with mixed-valence Mn^{3+} and Mn^{4+} are important components of the electrical structure of this sample. The catalytic activity of the investigated perovskites may be correlated with the presence of the active oxygen species (O^{2-}, O_2^-, O^-) determined by the structural defects generated due to high Mn^{4+}/Mn^{3+} ratio in the perovskite structure. This hole doping in the molecule shifts the Fermi level down, causing conduction and valence band behaviours [29]. Manganites are introduced as promising materials in optical devices due to the coexistence of electron and hole.

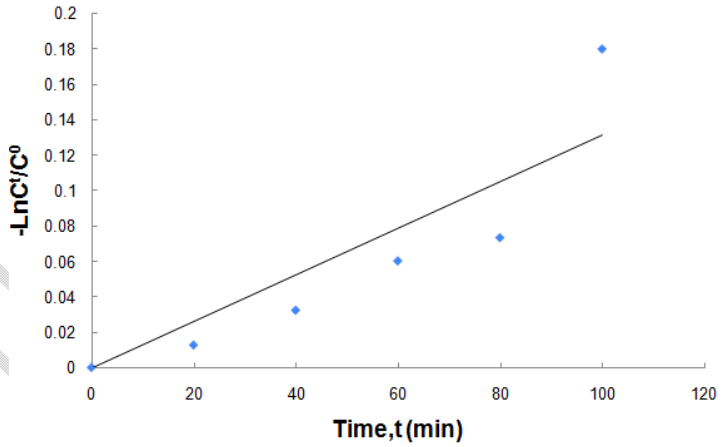

(Fig-11: Pseudo-first-order kinetics plot of MB degradation over $La_{0.75}Ca_{0.25}MnO_3$)

3.9. Photocatalysis mechanism:

An aqueous solution consisting of photocatalyst, air or oxygen, and Methylene blue as organic contaminant irradiated under visible light (hv), then electron–hole pairs are produced which were adsorbed on the photocatalyst surface and changes the process to produce OH radical[28]. The activated electron in conduction band also responds with oxygen molecule, that adsorbed on outer layer of photocatalyst to form superoxide radical. The photocatalytic mechanism can be given as:

$hv + Catalyst \rightarrow e^- + h^+$ [i]

The electron removed, reacts with oxygen present in water. As a result of which super-oxide radical ($O_2^{\cdot -}$) is produced.

$O_2 + e^- \rightarrow O_2^{\cdot -}$ [ii]

Then the holes generated in the VB of the catalyst now can directly oxidize MB, react with super-oxides radical, generating $OH^{\cdot}$ radicals. These $OH^{\cdot}$ predominantly causes the degradation of the chromophoric dye

$O_2^{\cdot -} + H^+ \rightarrow HOO^{\cdot}$ [iii]
$HOO^{\cdot} + e^- \rightarrow HO_2^-$ [iv]
$HOO^- + H^+ \rightarrow 2H_2O_2$ ($H_2O_2 = 2OH^-$) [v]
$Dye(MB) + OH^{\cdot}(Radical) \rightarrow CO_2 + H_2O + NH_4^+ + NO_3^- + Cl^-$ [vi]

The produced OH^- is very much essential for debasement of methylene blue dye from its aqueous solution. In the photodegradation mechanism, holes generated by light sources follow one electron oxidation path for the generation of hydroxyl radicals(OH^-). The generated OH radical react with methylene blue and forms CO_2, sulphate, nitrate,H_2O and HCl acid of little quantity.

4. CONCLUSION:

In this study $La_{0.75}Ca_{0.25}MnO_3$ nano perovskite was synthesized by a simple Sol-Gel method followed by pre-annealing/calcination at 800^0C. The acquired sample has a perovskite structure, according to XRD. SEM revealed micrometer-sized crystal particles that were randomly scattered. Using Tauc's equation, it was determined that the perovskite had a band gap energy value of 2.13 eV, which is within the range of photocatalyst behaviour when exposed to visible light. The photocatalyst behaviour of MB in aqueous solution was examined using visible light irradiation, which revealed efficient photocalytic activity. After 100 minutes of illumination, the photodegradation efficiency for decolorising MB solution (5ppm) by doped calcium manganite (0.07 gl^{-1}) was around 68.52%, with a reaction rate of 1.582 x10-3 min^{-1}.

REFERENCES

[1]. E. Murugan and R. Rangasamy**,** Development of Stable Pollution Free TiO_2/Au Nanoparticle Immobilized Green Photo Catalyst for Degradation of Methyl Orange, J. Biomed. Nanotechnol., (2011): 7: 225, DOI: https://doi.org/10.1166/jbn.2011.1277

[2]. B. Qi, Y. Hu, H. Liu, and Z. Dong, Photocatalytic Degradation and Toxic Effects of Ag-Doped ZnO Nanocrystallites J. Nanosci. Nanotechnol., (2011):11:9513. DOI:https://doi.org/10.1166/jnn.2011.5281

[3]. R. A. Carcel, L. Andronic, and A. Duta, Photocatalytic Degradation of Methylorange Using TiO_2, WO_3 and Mixed Thin Films Under Controlled pH and H_2O_2,J. Nanosci. Nanotechnol. (2011): 11:9095. DOI: https://doi.org/10.1166/jnn.2011.4283

[4]. M. A. Abdi, F. Djeffal, T. Bentrcia, and D. Arar, J. Nanosci. Nanotechnol. (2011):11: 9316. DOI: 10.1166/jnn.2011.4290

[5]. P. F. Du, L. X. Song, J. Xiong, Z. Q. Xi, J. J. Chen, L. H. Gao, and N. Y, Wang, High-efficiency photocatalytic degradation of methylene blue using electrospun ZnO nanofibers as catalyst. J. Nanosci. Nanotechnol, (2011):11:7723. DOI: 10.1166/jnn.2011.4733

[6]. Y. Tian, M. Fang, W. Xu, N. Li, Y. Chen, and L. Zhang, Kinetically controlled synthesis of bismuth tungstate with different structures by a NH4F assisted hydrothermal method and surface-dependent photocatalytic properties. J. Nanosci.Nanotechnol,(2011): 11:7802. DOI: 10.1016/j.jcis.2014.06.042

[7]. Singh R, Singh A, Misra V, Singh RP ;Degradation of Lindane contaminated soil using zero-valent iron nanoparticles. J. Biomed. Nanotechnol. (2011):7:175-176. DOI:10.1166/jbn.2011.1256.

[8]. Y. Yamin, N. M. Ismail, M. Z. Hussein, and N. Aminudin, J. Biomed.Nanotechnol, (2011): 7: 486
.

[9]. Serpone N, Emeline AV. Semiconductor Photocatalysis-Past, Present, and Future Outlook. The Journal of Physical Chemistry Letters, (2012) :3(5): 673-7. DOI: 10.1021/jz300071j

[10].Hernandez-Ramirez A, Medina-Ramirez I. Photocatalytic semiconductors: Springer; 2016

[11].T. Ji, F. Yang, Y. Lv, J. Zhou, and J. Sun, Photocatalytic and water-splitting properties of TiO_2 and Ag–TiO_2 films in the visible light region, J. Mater. Lett, (2009):63:2044. https://doi.org/10.1063/5.0058116

[12].Effect of doping manganese on photocatalytic performance of titania in degradation of rose Bengal rinku bairagi, meenakshi singh solanki and rakshit ameta, Int. J. Chem. Sci(2016): 14(4): 3237-3248

[13].T. Ohno, T. Tsubota, Y. Nakamura, and K. Sayama, Appl. Catal. A, (2005): 288:74.

[14].Methyl orange degradation using nano-$LaMnO_3$ as a green catalyst under the mild conditions Neda Rekavandi, Azim Malekzadeh, Elham Ghiasi, Nanochem Res, (2019):4(1):1-10, DOI: 10.22036/ncr.2019.01.001

[15].Photocatalytic Decomposition of Methyl Orange Over Nanosized Perovskite-Type Oxides Under Visible Light Irradiation Man Woo Ha, Won Young Jung, Kwon Taek Lim, Man Sig Lee, and Seong-Soo Hong, Journal of Nanoscience and Nanotechnology, (2013): 1: 2320–2324

[16].R. Spinicci, M. Faticanti, P. Marini, S. De Rossi, and P. Porta, "Catalytic activity of $LaMnO_3$ and $LaCoO_3$ perovskites towards VOCs combustion," Journal of Molecular Catalysis A: Chemical, (2003): 197: 147-155.

[17].N. Li, A. Boréave, J.-P. Deloume, and F. Gaillard, "Catalytic combustion of toluene over a Sr and Fe substituted LaCoO3 perovskite," Solid State Ionics, (2008): 179:1396-1400.

[18].R. D. Kumar, R. Thangappan, and R. Jayavel, "Enhanced visible light photocatalytic activity of LaMnO 3 nanostructures for water purification," Research on Chemical Intermediates, (2018): 44: 4323-4337,

[19].B. Barrocas, S. Sério, A. Rovisco, Y. Nunes, and M. M. Jorge, "Removal of rhodamine 6G dye contaminant by visible light driven immobilized Ca1- xLnxMnO3 (Ln= Sm, Ho; 0.1< x 0.4) photocatalysts," Applied Surface Science, (2016): 360:798-806,

[20].Sun M, Jiang Y, Li F, Xia M, Xue B and Liu D; Structure, Dye Degradation Activity and Stability of Oxygen Defective $BaFeO_{3-x}$ Mater.Trans. 51 **(**2010)1981

[21].A ARABI, M FAZLI and M H EHSANI , “Synthesis and characterization of calcium-doped lanthanum manganite nanowires as a photocatalyst for degradation of methylene blue solution under visible light irradiation”Bull. Mater. Sci., (2018): 41:1-8

[22].F. R. Afje and M. Ehsani, "Size-dependent photocatalytic activity of $La_{0.8}Sr_{0.2}MnO_3$ nanoparticles prepared by hydrothermal synthesis," Materials Research Express, 5,(2018) . **DOI** 10.1088/2053-1591/aaba51

[23]. M. Behpour and V. Atouf, "Study of the photocatalytic activity of nanocrystalline S, N-codoped TiO2 thin films and powders under visible and sun light irradiation," Applied Surface Science, (2012) :258:6595-6601,.

[24]. M. Shaterian, M. Enhessari, D. Rabbani, M. Asghari, and M. Salavati-Niasari, "Synthesis, characterization and photocatalytic activity of LaMnO3 nanoparticles," Applied Surface Science, (2014):318:213-217,

[25] A. Arabi, M. Fazli, and M. Ehsani, "Synthesis and characterization of calcium-doped lanthanum manganite nanowires as a photocatalyst for degradation of methylene blue solution under visible light irradiation," Bulletin of Materials Science, (2018) :41:77,.

[26] T. Larbi, M. Amara, B. Ouni, and M. Amlouk, "Enhanced photocatalytic degradation of methylene blue dye under UV-sunlight irradiation by cesium doped chromium oxide thin films,"Materials Research Bulletin, (2017) : 95:152-162,

[27]. Choi S G, Lee H S, Choi H, Chung S W and Park H H ; Thin Solid Films **(**2013): 529**:**352

[28] A. Franco, M. Neves, M.R. Carrott, M. Mendonça, M. Pereira, O. Monteiro, Photocatalytic decolorization of methylene blue in the presence of TiO_2/ZnS nanocomposites, J. Hazard. Mater. (2009): 161 (1) :545–550

[29]. S. Esmaeili, M.H. Ehsani, M. Fazli, Structural, optical and photocatalytic properties of La0.7Ba0.3MnO3 nanoparticles prepared by microwave method, Chemical Physics, (2020): 529: 110576 . https://doi.org/10.1016/j.chemphys.2019.110576